Electronic Supplementary Material (ESI) for Nanoscale.

Supporting Information

Self-Assembly of Spherical and Rod-Shaped Nanoparticles with full Positional Control

Julian A. Lloyd, , Yawei Liu, Soon Hock Ng, Thibaut Thai, Daniel E. Gómez, Asaph Widmer-Cooper and Udo Bach

DLVO Calculation Details

I. Model and Electrostatic Interaction

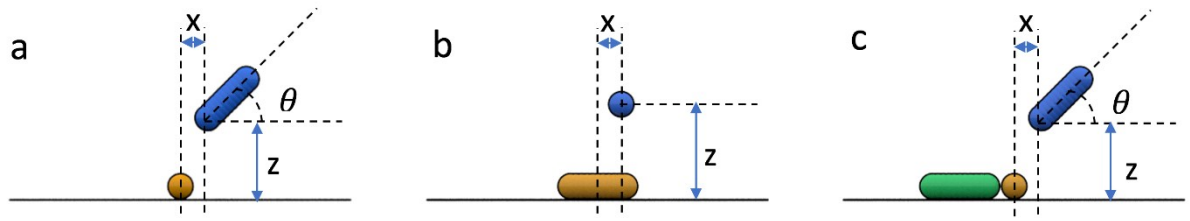

Fig. S1 Illustrations of the model systems for the DLVO calculations. (a) *Tip-on* assembly; (b) *On-top* assembly; (c) *In-the-gap* assembly.

In the DLVO calculations, the modified substrate was represented by a flat wall, the AuNP was modelled as a sphere, and the GNR was considered as a rigid linear chain of overlapping spheres (Figure S1). All spheres have the same diameter d. The number of consecutive spheres in the rod is $N = 11$, and the distance between them is fixed at $\Delta l = 0.2d$, so that the total length is $L = (N\text{-}1)\Delta l + d = 3d$.

Based on DLVO theory, the electrostatic interaction between two spheres is given by

$$E_{ss} = \frac{B_{ss}}{r} e^{-\kappa d(r-1)}$$

and between the sphere and the flat wall is given by

$$E_{sw} = B_{sw} e^{-\kappa d h}.$$

The dimensionless distances r and h denote the centre-to-centre distance between spheres and the distance between the wall surface and the sphere surface, respectively, both scaled by the

sphere diameter d. The constants B_{ss} and B_{sw} depend on the surface charge densities, the sizes of the spheres involved, and the electrolyte concentration of the surrounding solution:

$$B_{ss} = 4\pi\epsilon\epsilon_0(k_BT/e)^2a^2Y_sY_s$$

$$B_{sw} = 4\pi\epsilon\epsilon_0(k_BT/e)^2aY_sY_w$$

Here, a is the radius of the sphere ($a = 0.5d$), ϵ and ϵ_0 are the relative permittivity and the permittivity of vacuum, respectively. k_B is the Boltzmann constant, T is the temperature, e is the unit charge of an electron and Y is the scaled effective surface potential for the involved sphere or wall.

The inverse screening length, κ, is given by

$$\kappa = \left(\frac{e^2I}{\epsilon\epsilon_0k_BT}\right)^{1/2}$$

with I the ionic strength.

In our calculations, we assumed that the rod has an approximately constant surface charge density, which seems reasonable given that the charge comes from ligands that should be distributed close to evenly across the surface of the GNR. This means that a spherical particle should feel a nearly uniform electrostatic field around the rod as a function of distance from the rod surface. This situation was roughly achieved by only considering electrostatic interactions with the two spheres located at the ends of the rod. For example, Fig. S2 gives the interaction energy between a rod and a sphere at $B_{sr} = -1.5/2$, $\kappa d = 0.3$, showing the nearly uniform electrostatic field around the rod.

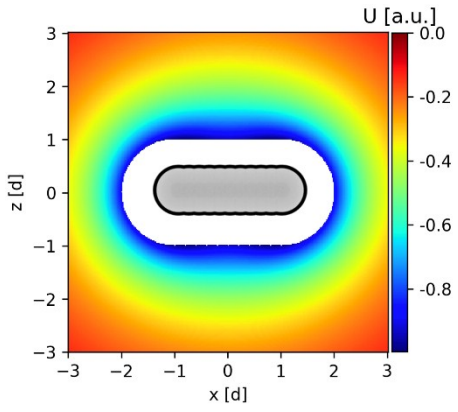

Fig. S2 The interaction energy U (in arbitrary units) between a rod and a sphere at $B_{sr} = -1.5/2$ and $\kappa d = 0.3$. The gray illustration shows a rod consisting of 11 overlapping spheres.

We used the parameters from the study by Zheng *et al.*[1] to estimate the relative value of B and κd for our calculations. To confirm our model, we reproduced their Figure 1a,[1] which is an

example of the interaction energies between a $30\,nm$ positively charged AuNP and a $30\,nm$ negatively charged AuNP on a substrate with ionic strength ~$13.3\,\mu M$. As $Y_s \approx 3Y_w$ for the AuNP and the substrate, we approximately have $B_{ss}/B_{sw} = aY_s/Y_w \approx 1.5$. The calculated result with $B_{ss} = -1.5$, $B_{sw} = 1.0$, $\kappa d = 0.36$ is given in Fig. S3. We obtain an energy barrier of 0.11 at a separation of $4.25d$, which is very close to the previously reported value of $0.096\,eV$ at a separation of $120\,nm$ (i.e., at $4d$).

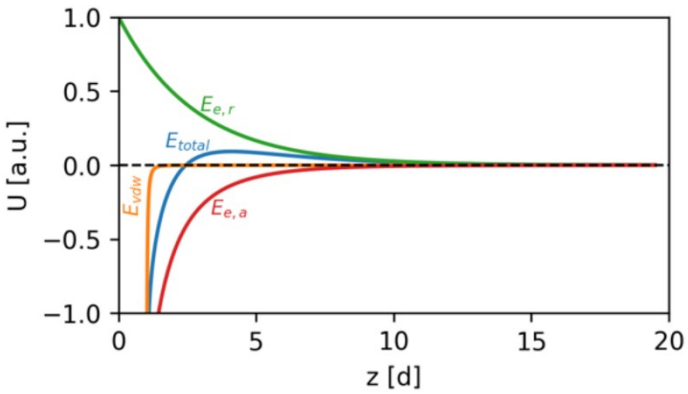

Fig. S3 Interaction energies between a positively charged AuNP and a negatively charged AuNP on a silica-coated silicon substrate (ionic strength ~$13.3\,\mu M$). Our calculations are consistent with those reported by Zheng *et al.* $E_{e,r}$ is the electrostatic repulsion energy between the approaching AuNP and the substrate; $E_{e,a}$is the electrostatic attraction energy between the approaching AuNP and surface-confined AuNP; E_{vdW} is the van der Waals interaction energy between the approaching AuNP and the substrate; and z is the particle–substrate distance.

II. Calculations for different assembly pathways

A. Tip-on assembly

In the calculations for the *tip-on* assembly, we need B_{sr} for the rod-sphere interaction, and B_{rw} for the rod-wall interaction. The value of Y_s for the rod does not affect the ratio of B_{sr} to B_{rw}. Hence, according to the estimation in Fig. S3, we set $B_{sr} = -1.5/2$ and $B_{rw} = 1.0/2$. For κd, the example in Fig. S3 gives a reference value of $\kappa d = 0.36$ for a $30\,nm$ AuNP at ionic strength ~13.3 μM. Therefore, to analyze interactions involving the smaller $20\,nm$ particles in our experiments at NaCl concentrations of 20, 80, 115 and 230 μM, κd was set to be 0.3, 0.6, 0.7 and 1.0.

We calculated the electrostatic interaction energies for the rod at different positions and orientations. As shown in Figure S1a, the position of the rod is represented by the location of the end-sphere with respect to the sphere on the wall/substrate, (x, z), and the orientation is represented by the angle, $\theta = 0{\sim}180°$. Fig. S4a shows an example of the calculated results at $\kappa d = 0.7$ $(\sim 115\ \mu M)$ when the rod approaches the wall with the position fixed at $x = 0$ At each value z the orientation of $\theta = 90°$ always corresponds to the local minimum of the interaction energy, indicating the rod prefers to be perpendicular to the wall. Fig. S4b shows the interaction energy corresponding to the favored orientation at each position. Obviously, during the assembly process, an energy barrier has to be overcome. In our calculations, the energy barrier is smallest when the rod approaches the wall with $x = 0$ at an angle perpendicular to the wall.

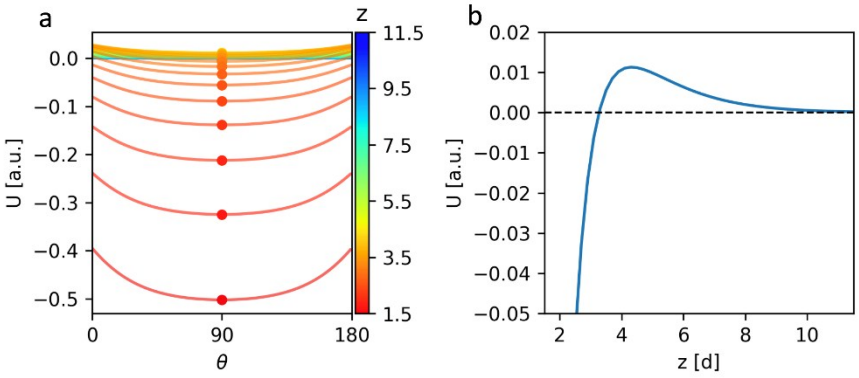

Fig. S4 (a) Interaction energy between a rod and a sphere sitting on the wall/substrate at selected distances and orientations when $\kappa d = 0.7$ $(\sim 115\ \mu M)$ and $x = 0$. The circle symbols indicate the local minimum of energy at each value of z. (b) The interaction energy corresponding to the favored orientation at each value of z.

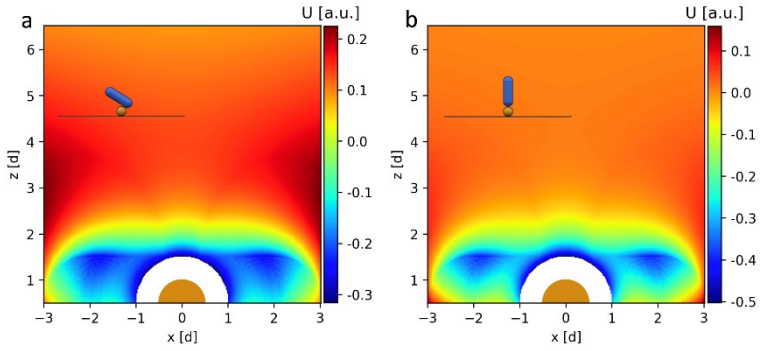

Fig. S5 Interaction energies for the favored orientation at different positions when a) $\kappa d = 0.3(\sim 20\ \mu M)$ and b) $\kappa d = 0.7(\sim 115\ \mu M)$. The inserts illustrate the position and the orientation of the rod corresponding to the global minimum of energy.

B. On-top assembly

We calculated the electrostatic interaction energies for the sphere at different positions, (*x, z*) (main manuscript, Fig. 2b). In the calculations, we set $B_{sr} = -1.5/2$, $B_{sw} = 1.5$. For κd, we set it to be 1.3 according to the ionic strength ~400 μM.

C. Trimer assembly

We calculated the electrostatic interaction energies for the rod at different positions and orientations (main manuscript, Fig. 2c). In the calculations, we set $B_{sr} = -1.5/2$ and $B_{rw} = 1.0/2$, and $B_{rr} = 1.0/4$. For the value of κd, we set it to be 0.8 according to the ionic strength ~150 μM.

Dimer assemblies with different materials

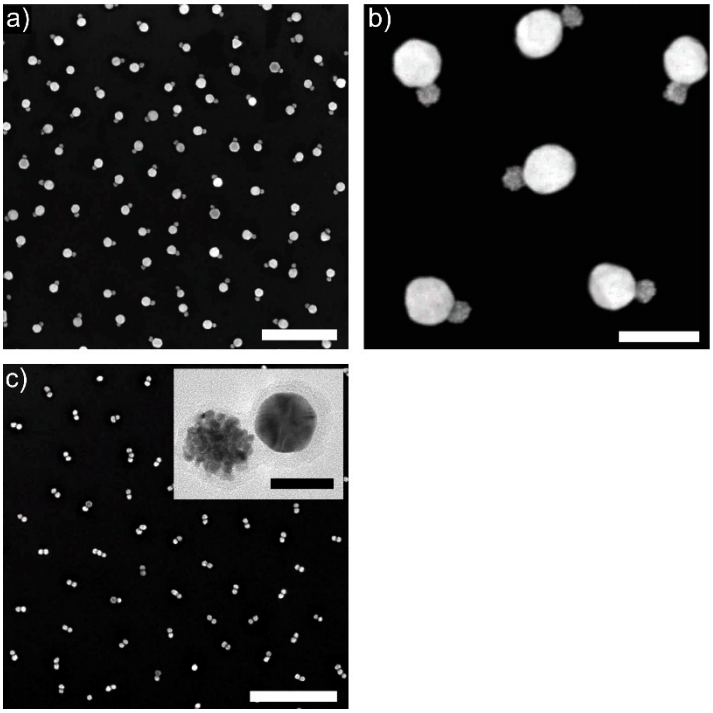

Fig. S6: SEM micrographs of Au-Pt hetero-structures assembled via electrostatic assembly. a) Overview image of a high yield dimer assembly with 60 nm AuNPs and 30 nm PtNPs (scale bar 500 nm). b) High resolution SEM image of the same assemblies (scale bar: 100 nm). c) Overview image of a dimer assembly with 30 nm AuNPs and 30 nm PtNPs (scale bar 500 nm). Inset: TEM image of a single Pt-Au dimer (scale bar: 30 nm).

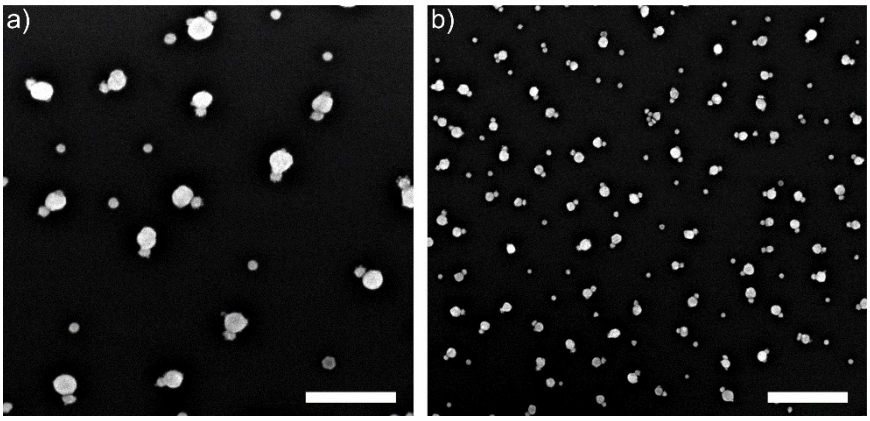

Fig. S7: SEM images of Au-Ag hetero-dimer assemblies. a) High resolution SEM micrograph of 60 nm AgNPs assembled on 30 nm AuNPs (scale bar: 250 nm). b) Overview SEM image of the same assemblies (scale bar: 500 nm).

Additional SEM images and statistics

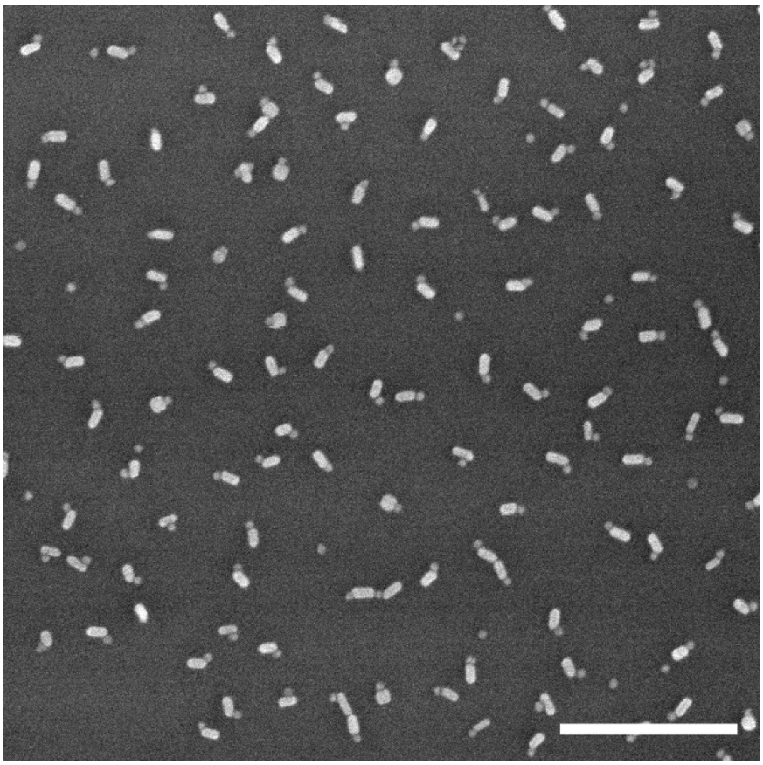

Fig. S8 SEM micrograph of an average tip-on assembly at optimized conditions in step 2. 3 h incubation time, 30 ºC assembly temperature, a 115 µM NaCl concentration and vertical drying in air after dip-washing (scale bar: 500 nm).

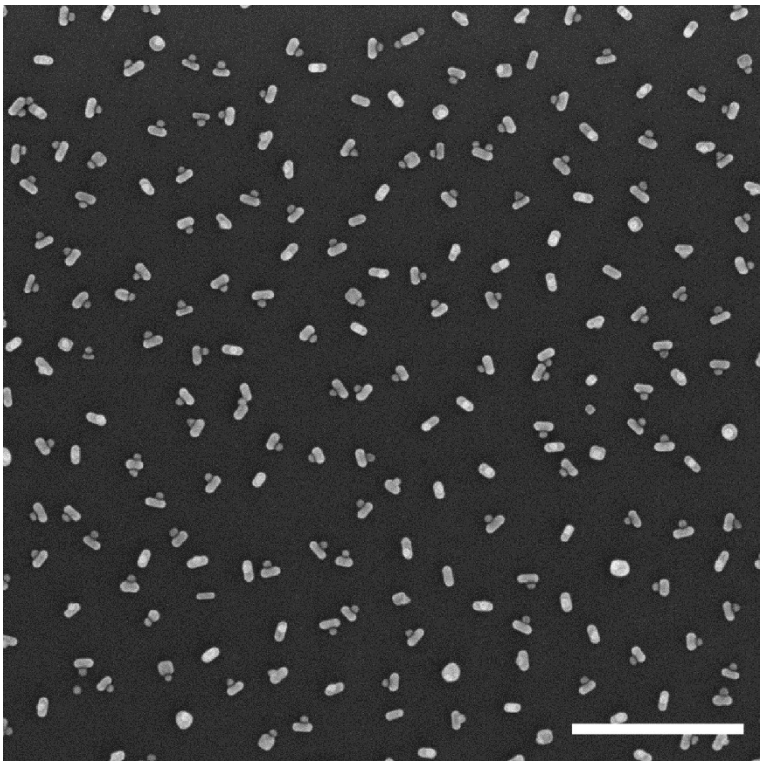

Fig. S9 SEM micrograph of a *side-on* assembly (scale bar: 500 nm). After an initial assembly of the GNRs in step 1, the optimized conditions for step 2 are: 3 h incubation time, 25 ºC assembly temperature, a 400 μM NaCl concentration and vertical drying in air after dip-washing.

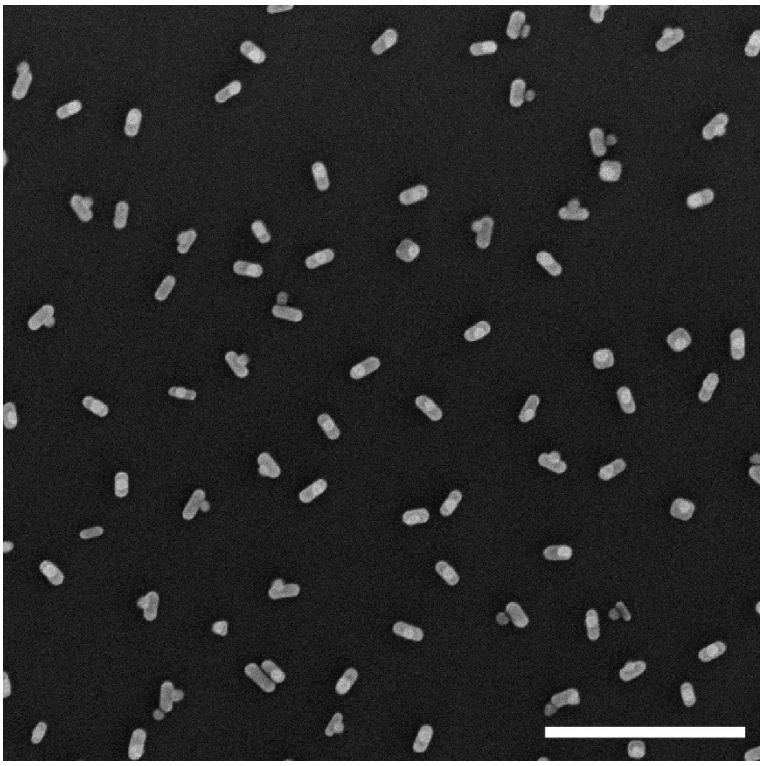

Fig. S10 SEM micrograph of an *on-top* assembly (scale bar: 400nm). Assembly conditions are the same as for the *side-on* assembly, except for the drying step: here, the assemblies are blow-dried under a stream of nitrogen after dip-washing in step 2.

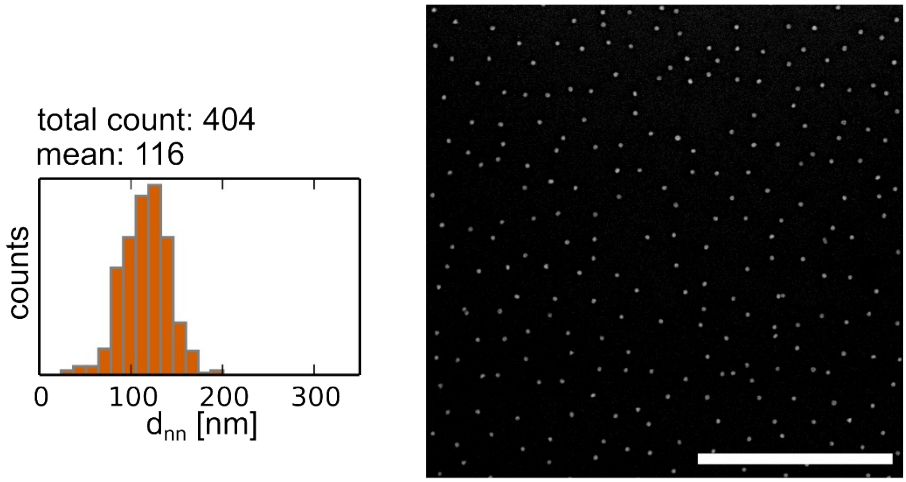

Fig. S11 Left: nearest neighbor distribution of the step 1 assembly of negatively charged AuNPs on a positively charged substrate. Right: SEM image of such assembly (scale bar: 1 µm).

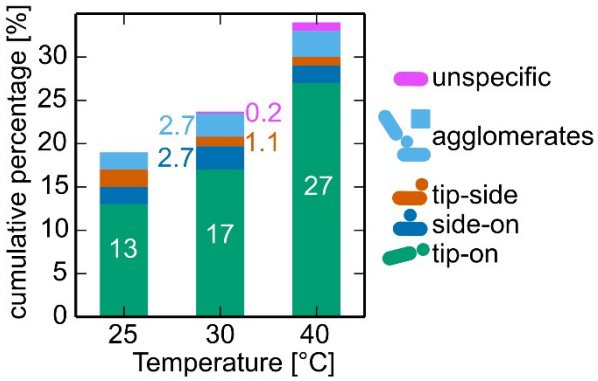

Fig. S12 Statistics of the different observed structures after step 2 (starting with a substrate of immobilized AuNPs) for *tip-on* assembly results. The temperature of the assembly solution in step 2 was varied between 25 ºC and 40 ºC. The incubation time was 3 h, no NaCl was added to the solution. Pictograms on the right indicate the different motifs. Individual AuNPs on the substrate without any GNR attached are not shown here for clarity. They make up the remaining part to reach 100%.

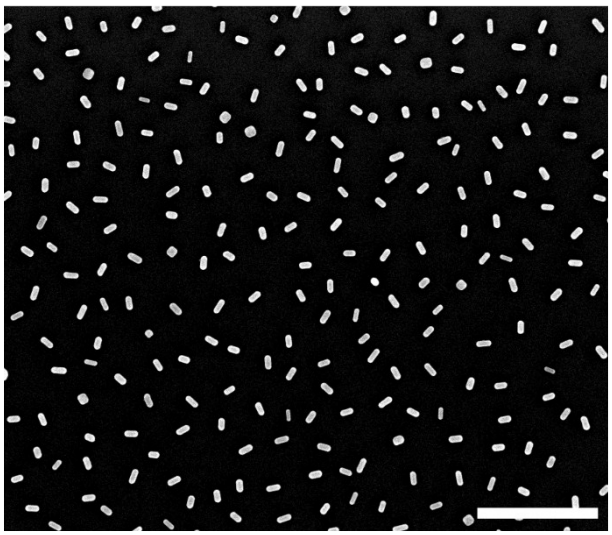

Fig. S13 SEM image of positively charged GNRs assembled on a negatively charged SiO_2/Si substrate (scale bar: 500 nm).

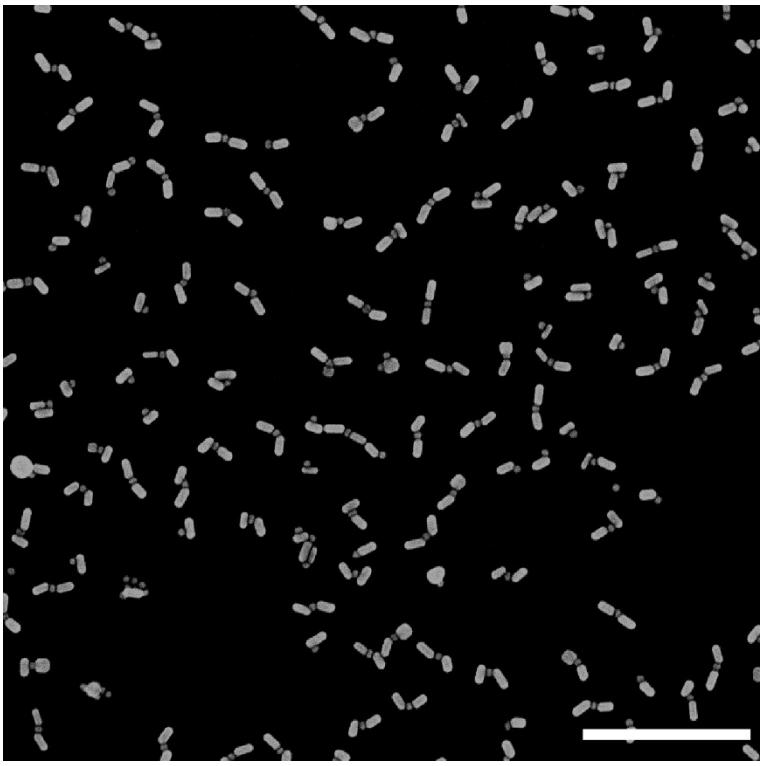

Fig. S14: SEM micrograph of an *in-the-gap* assembly (scale bar: 500 nm). Assembly conditions of step 2 were as follows: 3 h incubation time, 30 ºC assembly temperature, a 115 μM NaCl concentration and vertical drying in air after dip-washing. The same conditions where used for step 3.

References:

(1) Y. Zheng, L. Rosa, T. Thai, S. H. Ng, D. E. Gómez, H. Ohshima, U. Bach, *J. Mater. Chem. A,* 2015, ***3***, 240–249.